Photoresponsive Spiropyran-Functionalised MOF-808: Postsynthetic Incorporation and Light Dependent Gas Adsorption Properties

SCHOLARONE™
Manuscripts

Journal Name

COMMUNICATION

Photoresponsive Spiropyran-Functionalised MOF-808: Postsynthetic Incorporation and Light Dependent Gas Adsorption Properties

Katherine Healey,[a] Weibin Liang,[a] Peter D. Southon,[a] Tamara L. Church,[a] Deanna M. D'Alessandro[a*]

The first example of spiropyran-incorporated metal-organic framework was synthesised *via* a two-step post-synthesis modification of the Zr-oxo nodes in MOF-808. The incorporated spiropyran could not otherwise be obtained *via* the analogous one-step *de novo* synthesis. The resulting MOF-808-SP showed a photoresponsive surface area, pore volume and CO_2 uptake, relevant for light-dependent gas separations processes.

Spiropyrans are a group of photoactive molecules with two orthogonal π-networks connected *via* a central tetrahedral carbon (C_{spiro}).[1-4] The nonbonding N p_x orbital in the spiropyran molecule can donate electron density into the C_{spiro}–O antibonding orbital, though this effect is partially offset by the similar donation of the O nonbonding orbital into the C_{spiro}–O orbital.[5] When triggered by UV irradiation, a $2\pi + 2\pi + 2\pi$ pericyclic reaction occurs, cleaving the C_{spiro}–O bond in the colourless spiropyran and leading to interconversion to the coloured merocyanine (MC) form.[5] Upon visible light and/or heat exposure, the MC molecule reverts back to its original spiropyran form (Fig. 1).[1] The ring-closing reaction rate for MCs is highly sensitive to the R^2 substitution, and falls in the range of 10^{-6} to 10^0 s^{-1}.[6]
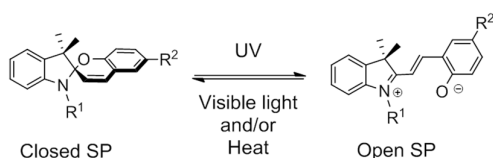

Fig. 1 Molecular demonstration of the reversible isomerisation between spiropyran and merocyanine.

Metal-organic frameworks (MOFs) are a class of multi-dimensional porous networks composed of organic struts and inorganic nodes, and can be systematically tuned in terms of chemical composition and precise arrangement.[7-9] Recently, there has been a significant interest in developing photoresponsive MOFs for light-modulated guest separation/storage; this process offers a potential low-energy alternative for post-combustion flue gas separation.[10-12] These studies have focused extensively on azobenzene frameworks,[13-19] as well as on diarylethenes[20, 21] and others.[10, 22] As a photochromic moiety, spiropyrans in MOFs are understudied, with only one example reported to date, for a MOF incorporating a non-covalently impregnated spiropyran.[23] Using a microwave-assisted crystallisation inclusion method, 8–9 wt% of nitrobenzospiropyran was introduced as a guest in the cavities of the indium MOF ($[In_3O(OH)(btc)_2]\cdot 2H_2O$, JUC-120, btc = 1,3,5-benzenetricarboxylate) to form a hybrid material with highly reversible photochromism.[23] Besides host-guest chemistry, incorporation of spiropyran molecules onto the metal clusters *via* postsynthetic modification (PSM) serves as a promising approach to introduce photochromism into MOF materials.[24]

In the present study, a novel spiropyran with a short-chain carboxylic acid (acetate) and a nitro group positioned at R^1 and R^2, respectively, was designed and targeted (*2-(3',3'-dimethyl-6-nitrospiro-[chromene-2,2'-indolin]-1'yl)acetic acid,* SP). The carboxylate functionality on the R^1 position was employed to facilitate spiropyran appendage to the metal clusters; the electron-withdrawing nitro group in R^2 position enabled the designed spiropyran to undergo isomerisation *via* a lower energy triplet pathway, in turn permitting faster and more efficient interconversion.[5]

The zirconium-based MOF-808[25, 26] (Fig. 2a, $[Zr_6O_4(OH)_4(btc)_2(HCOO)_6]$) was chosen as a PSM platform for the following reasons: 1) the high oxidation state of Zr^{IV} enables strong metal-ligand bonds, making MOF-808 highly chemically robust, and thus permitting the installation and further chemical modification of the spiropyran functional groups;[27-30] 2) MOF-808 possesses sufficiently large cavities to accommodate the SP molecule (*ca.* 14 Å for SP length and *ca.* 18.4 Å for pore diameter in MOF-808);[25, 26] 3) the relatively labile formate ligands on the Zr_6 cluster in MOF-808 are

a. School of Chemistry, Building F11, The University of Sydney, NSW 2006, Australia.
Corresponding author email: deanna.dalessandro@sydney.edu.au

available for chemical modification of the cavities *via* solvent-assisted ligand exchange (SALE).[31, 32] Herein we also report the novel synthesis of a spiropyran through multi-step PSM *inside* MOF-808, and explore the guest sorption properties of the resulting photoactive framework. A combination of X-ray powder diffraction (XRPD), gas adsorption measurements, and Fourier transform infrared (FTIR), UV-vis, and nuclear magnetic resonance (NMR) spectroscopies were employed to interrogate the potential light-dependent properties of the functionalised MOF.
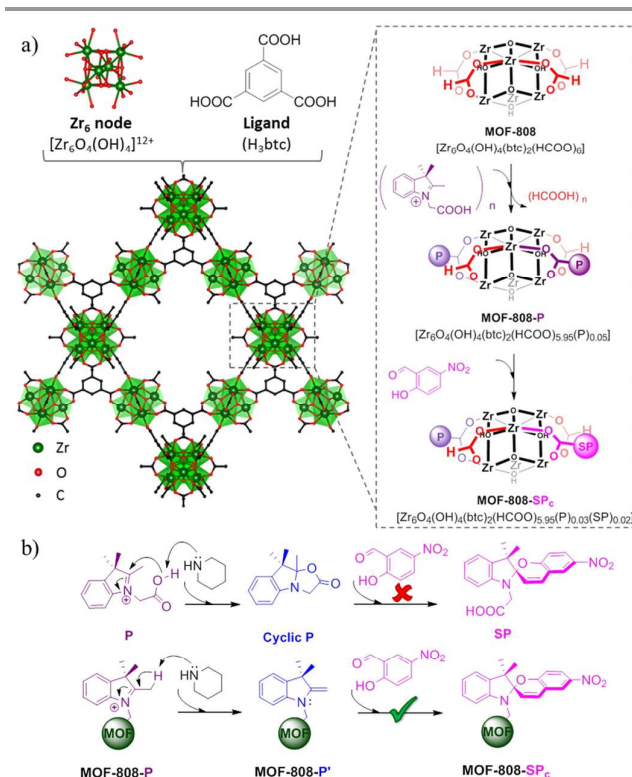

Fig. 2 (a) Molecular representation of MOF-808 (left) and the schematic representation of the solvent-assisted ligand exchange (SALE) of the *1-(carboxymethyl)-2,3,3-trimethyl-3H-indol-1-ium* (P) molecules and the subsequent secondary functionalisation reaction for the synthesis of *2-(3',3'-dimethyl-6-nitrospiro-[chromene-2,2-indolin]-1'yl) acetate* (SP, right) on the Zr-oxo clusters in MOF-808; (b) Proposed mechanism showing intramolecular electrophilic attack preventing the synthesis of SP in solution (top) and SP synthesis mechanism *via* SALE and secondary functionalization reaction in MOF-808 (bottom).

Although the synthesis of 3-(3',3'-dimethyl-6-nitrospiro[chromene-2,2'-indolin]-1'-yl)propanoic acid has been reported previously,[33-35] initial attempts to synthesise the SP with an acetate functionality using a typical synthetic procedure for R_1-substituted spiropyrans[33] was unsuccessful. We suspected that the short acetate functionality in 1-(carboxymethyl)-2,3,3-trimethyl-3H-indol-ium iodide (P) favoured intramolecular electrophilic attack for the subsequent formation of 9,9,9a-trimethyl-9,9a-dihydrooxazolo[3,2-a]indol-2(3H)-one (cyclic P), which precluded the formation of desired SP (Fig. 2b). Our hypothesis was confirmed by the NMR and FTIR analysis. After the bulk reaction, the product was separated from the precursors by column chromatography. ^{1}H and ^{13}C NMR measurements qualitatively indicated the presence of cyclic P as the major product in the reaction mixture (ESI). In addition, compared to P, the FTIR spectrum of cyclic P shows a change in both the C–O (1726 cm^{-1} to 1717 cm^{-1}) and C=O (1186 cm^{-1} to 1287 cm^{-1}) vibrations and a disappearance of the O–H (2900 cm^{-1}) stretch, indicating the formation of an ester in cyclic P (ESI). In order to synthesise SP the intramolecular cyclisation of P must be prevented. Thus in the following experiments, we attempted to append the acetate group of P onto the Zr_6 cluster in MOF-808 *before* performing the SP reaction (Fig. 2). In this approach, steric effects resulting from appendage would prevent intramolecular cyclisation and allow the desired condensation reaction to proceed (Fig 2b). In a typical experiment, MOF-808 (397 mg) and P (0.148 mg) were soaked in 10 mL *N,N'*-dimethylformamide (DMF) overnight at room temperature to enable SALE, following which MOF-808-P was soaked in fresh DMF to remove unreacted ligands. Thereafter, the sample was solvent-exchanged with ethanol and dried *in vacuo* (Fig. 2a and ESI). The extent of P incorporation in MOF-808-P was estimated by ^{1}H NMR spectroscopy after dissolving the framework in KOH/D_2O.[26] The corresponding signals of the incorporated P were integrated against that of the btc ligands.[26] This information, coupled with elemental analysis, allowed the chemical formula of MOF-808-P to be assigned as $[Zr_6O_4(OH)_4(btc)_2(HCOO)_{5.95}(P)_{0.05}]$. MOF-808-P was then further chemically modified to form MOF-808-SP ($[Zr_6O_4(OH)_4(btc)_2(HCOO)_{5.95}(P)_{0.03}(SP)_{0.02}]$) *via* a condensation reaction with 2-hydroxy-5-nitrobenzaldehyde (Fig. 2b and ESI). Considering that the cavity size in MOF-808 is 16.6 Å, the theoretical ratio of spiropyran (~14.9 x 8.5 x 7 Å)[23] incorporation is 1 spiropyran per pore (or per 2 Zr_6 clusters) (see ESI for calculations). Thus, the actual incorporation SP was low with respect to the maximum amount that would be possible.

After PSM, the XRPD patterns of both MOF-808-P and MOF-808-SP showed no signs of degradation of the parent frameworks (ESI);[9, 26] slight differences in relative diffraction peak intensities were observed, and may be attributed to changes in the electron density introduced by the P or SP ligands. The successful incorporation of P and the formation of SP in MOF-808-P and MOF-808-SP, respectively, were initially evidenced by their optical change. Compared to MOF-808, which has a white appearance, MOF-808-P attains a pink colouration after SALE, and further changes to red upon condensation to give MOF-808-SP. These results were qualitatively confirmed by UV-vis spectroscopy measurements (Fig. 3b). Compared to the spectra of MOF-808, distinctive new adsorption bands centred at 18100 and 27980 cm^{-1} appear in those of MOF-808-P and MOF-808-SP, respectively, which can be attributed to the ligand-to-cluster charge transfer (LCCT) interaction between the highest occupied molecular orbital (HOMO) of the introduced moiety and the *d* orbitals in Zr^{IV} (Fig. 3b).[36] In this case, Zr^{IV} (d^0) is a good electron acceptor, while P and SP are strong π-donors; so the energy of the HOMO reflects the extent of π-delocalisation in the incorporating molecules. Compared to SP, P has only one delocalised

aromatic system, which results in a lower energy LCCT. Ligand-to-metal charge transfer (LMCT) systems involving spiropyrans and with similar UV-vis spectra have previously been reported.[37-39]

The Ar adsorption isotherms of MOF-808-P and MOF-808-SP retain the type IVb shape[40] (with a step at $p/p_0 \approx 0.05$, Fig. 2c) found for the MOF-808. Brunauer–Emmett–Teller (BET) analyses of the adsorption isotherms indicate a decrease in surface area from 1201 $m^{-1} g^{-1}$ for MOF-808 to 857 and 836 $m^{-1} g^{-1}$ for MOF-808-P and MOF-808-SP, respectively, which is expected as a result of guest incorporation and its further chemical modification. As additional evidence of P and SP incorporation, non-local density functional theory calculations (DFT, based on the *DFT-Ar on oxides@87 K model* in the MicroActive software, Micromeritics Instruments Inc.) show a reduction in the total pore volume for the 16 Å cavities in the MOFs-808-P and MOF-808-SP, though no drastic changes were found in the average pore sizes (ESI). CO_2 adsorption analysis indicated that MOF-808-SP exhibited a significantly higher CO_2 affinity than the parent MOF-808 (ESI). It is proposed that the N and O on the introduced SP moieties can improve the thermodynamic interaction between CO_2 and the framework pore environment. This result was supported by a recent computational study demonstrating that CO_2 interacts more strongly with N-containing heterocycles and NO_2 groups than its aromatic interaction with btc.[41]

The isomerisation of SP inside MOF-808-SP (Fig. 3a) was further investigated through a range of techniques. The UV-vis spectrum of MOF-808-SP after UV irradiation showed a blue-shifted (27980 to 28750 cm^{-1}) LCCT band, which can be explained by the increase in conjugation resulting from SP to MC isomerisation.[5] Variable temperature (VT) UV-vis spectroscopy was used to further probe the change of the LCCT band in MOF-808-SP (ESI). It was predicted that an increase in temperature (50 °C)[5] would cause the MC form to reverse back to the SP form, shifting the LCCT band to its energy prior to UV irradiation. However, for MOF-808-SP, an increase in temperature resulted in a further blue-shift of the LCCT absorption, indicating that heat favours the ring opening reaction (ESI). A similar phenomenon was reported for the host-guest system with JUC-120 and SPs,[23] and was attributed to the stabilisation of the polar merocyanine from in the pore environment. That was also possible for MOF-808-SP due to the presence of polar Zr-OH groups in the Zr_6 clusters.[42] In addition, MOF-808-SP shows a decrease in BET value after UV irradiation (639 $m^3 g^{-1}$, Fig. 3c), indicating a change in the framework pore environment. Non-local density functional theory calculations (conducted using the MicroActive software, Micromeritics Instruments Inc.) demonstrated a decrease in the large pore volume for MOF-808-SP after UV irradiation (ESI), which is attributed to the increased size of MC.[5] In principle, after UV-irradiation, the MOF-808-SP should show a stronger CO_2 affinity due to potential interactions between CO_2 and the charged moieties present in the open MC form (Fig. 3a). However, quantitative calculation of the heat of CO_2 adsorption was prevented by the gradual isomerisation of the incorporated SP during the measurement of sequential CO_2 isotherms at 25-45 °C. Instead, successive CO_2 isotherms were measured at 298 K for MOF-808-SP to demonstrate the change in CO_2 uptake before and after isomerisation (Fig. 3d). After UV irradiation, the CO_2 capacity of MOF-808-SP increased from 1.34 to 1.57 mmol g^{-1} at 1.2 bar (Fig. 3d). In all, both UV-vis and gas-adsorption studies confirm the photoresponsive nature of MOF-808-SP.

In summary, a new photoactive framework incorporating spiropyrans was synthesised *via* a two-step post-synthesis modification, whereby the SP condensation reaction was performed after appendage of P to the Zr_6 node of MOF-808. SP could not be similarly obtained *via* bulk synthesis. MOF-808-SP showed a photoresponsive BET surface area, pore volume and CO_2 uptake, demonstrating its potential for light dependent low energy gas separation and/or storage. In addition, the present study provides an important proof-of-concept example of the photoresponsive nature of spiropyran-functionalised MOFs, leading the way towards other framework platforms that may also exhibit light modulated properties.
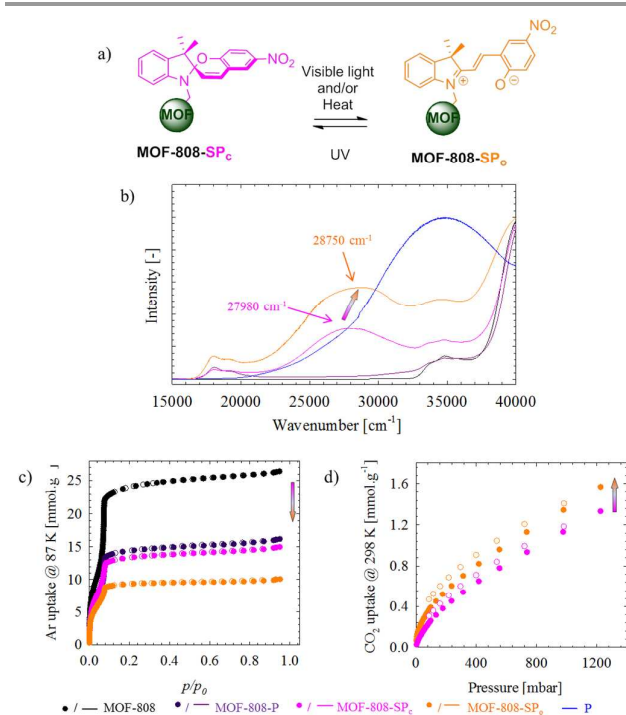
Fig. 3 a) Schematic representation of the photoisomerisation of MOF-808-SP; b) UV-vis spectra for MOF-808 (black), P (blue), MOF-808-SP (pink), and MOF-808-SP after UV irradiation (orange, λ = 254 nm, 30 min); c) Ar adsorption (filled) and desoption (open) isotherms for MOF-808 (black), MOF-808-P (purple), MOF-808-SP (pink) and MOF-808-SP after 30-min UV irradiation (orange); d) CO_2 adsorption (filled) and desorption (open) isotherms for MOF-808-SP and MOF-808-SP after 30-min UV irradiation.

Notes and references

1 J. A. Young, Farmer, B.L., Adams, W.W, Spectrum and Structure of Spiropyran, University of Virginia, Department of Materials Science, 1994.
2 P. K. Kundu, D. Samanta, R. Leizrowice, B. Margulis, H. Zhao, M. Börner, UdayabhaskararaoT, D. Manna and R. Klajn, Nat Chem, 2015, 7, 646-652.
3 M. Irie, Chem. Rev., 2000, 100, 1683-1684.
4 R. Heiligman-Rim, Y. Hirshberg and E. Fischer, J. Phys. Chem., 1962, 66, 2470-2477.
5 V. I. Minkin, Chem. Rev., 2004, 104, 2751-2776.
6 E. Berman, R. E. Fox and F. D. Thomson, J. Am. Chem. Soc., 1959, 81, 5605-5608.
7 N. Stock and S. Biswas, Chem. Rev., 2011, 112, 933-969.
8 T. Devic and C. Serre, Chem. Soc. Rev., 2014, 43, 6097-6115.
9 H. Furukawa, K. E. Cordova, M. O'Keeffe and O. M. Yaghi, Science, 2013, 341, 974.
10 1S. Castellanos, F. Kapteijn and J. Gascon, CrystEngComm, 2016, Ahead of Print.
11 F.-X. Coudert, Chem. Mater., 2015, 27, 1905-1916.
12 A. Das and D. M. D'Alessandro, CrystEngComm, 2015, 17, 706-718.
13 J. W. Brown, B. L. Henderson, M. D. Kiesz, A. C. Whalley, W. Morris, S. Grunder, H. Deng, H. Furukawa, J. I. Zink, J. F. Stoddart and O. M. Yaghi, Chem. Sci., 2013, 4, 2858-2864.
14 J. Park, L.-B. Sun, Y.-P. Chen, Z. Perry and H.-C. Zhou, Angew. Chem., Int. Ed., 2014, 53, 5842-5846.
15 A. Modrow, D. Zargarani, R. Herges and N. Stock, Dalton Trans., 2011, 40, 4217-4222.
16 L. L. Gong, X. F. Feng and F. Luo, Inorg. Chem., 2015, 54, 11587-11589.
17 R. Lyndon, K. Konstas, B. P. Ladewig, P. D. Southon, C. J. Kepert and M. R. Hill, Angew. Chem., Int. Ed., 2013, 52, 3695-3698.
18 J. Park, D. Yuan, K. T. Pham, J.-R. Li, A. Yakovenko and H.-C. Zhou, J. Am. Chem. Soc., 2012, 134, 99-102.
19 S. Castellanos, A. Goulet-Hanssens, F. Zhao, A. Dikhtiarenko, A. Pustovarenko, S. Hecht, J. Gascon, F. Kapteijn and D. Bleger, Chem. - Eur. J., 2016, 22, 746-752.
20 I. M. Walton, J. M. Cox, J. A. Coppin, C. M. Linderman, D. G. Patel and J. B. Benedict, Chem. Commun., 2013, 49, 8012-8014.
21 J. Park, D. Feng, S. Yuan and H.-C. Zhou, Angew. Chem., Int. Ed., 2015, 54, 430-435.
22 22. C. L. Jones, A. J. Tansell and T. L. Easun, J. Mater. Chem. A, 2015, Ahead of Print.
23 F. Zhang, X. Zou, W. Feng, X. Zhao, X. Jing, F. Sun, H. Ren and G. Zhu, J. Mater. Chem., 2012, 22, 25019-25026.
24 O. Karagiaridi, W. Bury, J. E. Mondloch, J. T. Hupp and O. K. Farha, Angew. Chem., Int. Ed., 2014, 53, 4530-4540.
25 H. Furukawa, F. Gandara, Y.-B. Zhang, J. Jiang, W. L. Queen, M. R. Hudson and O. M. Yaghi, J. Am. Chem. Soc., 2014, 136, 4369-4381.
26 W. Liang, H. Chevreau, F. Ragon, P. D. Southon, V. K. Peterson and D. M. D'Alessandro, CrystEngComm, 2014, 16, 6530-6533.
27 S. Yuan, Y.-P. Chen, J. Qin, W. Lu, X. Wang, Q. Zhang, M. Bosch, T.-F. Liu, X. Lian and H.-C. Zhou, Angew. Chem., Int. Ed., 2015, 54, 14696-14700.
28 D. Feng, K. Wang, J. Su, T.-F. Liu, J. Park, Z. Wei, M. Bosch, A. Yakovenko, X. Zou and H.-C. Zhou, Angew. Chem., Int. Ed., 2015, 54, 149-154.
29 S. Yuan, W. Lu, Y.-P. Chen, Q. Zhang, T.-F. Liu, D. Feng, X. Wang, J. Qin and H.-C. Zhou, J. Am. Chem. Soc., 2015, 137, 3177-3180.
30 P. Deria, W. Bury, J. T. Hupp and O. K. Farha, Chem. Commun., 2014, 50, 1965-1968.
31 R. C. Klet, Y. Liu, T. C. Wang, J. T. Hupp and O. K. Farha, J. Mater. Chem. A, 2016, 4, 1479-1485.
32 S.-Y. Moon, Y. Liu, J. T. Hupp and O. K. Farha, Angew. Chem., Int. Ed., 2015, 54, 6795-6799.
33 X. Li, Y. Wang and T. Matsuura, J. Meng, Heterocycles, 1999, 51, 2639-2651.
34 H. R. Allcock and C. Kim, Macromolecules, 1991, 24, 2846-2851.
35 D. Liu, W. Chen, K. Sun, K. Deng, W. Zhang, Z. Wang and X. Jiang, Angew. Chem., Int. Ed., 2011, 50, 4103-4107, S4103/4101-S4103/4116.
36 W. Liang, R. Babarao and D. M. D'Alessandro, Inorg. Chem., 2013, 52, 12878-12880.
37 K. Hakouk, O. Oms, A. Dolbecq, J. Marrot, A. Saad, P. Mialane, H. El Bekkachi, S. Jobic, P. Deniard and R. Dessapt, J. Mater. Chem. C, 2014, 2, 1628-1641.
38 M. L. Macnaughtan, H. S. Soo and H. Frei, J. Phys. Chem. C, 2014, 118, 7874-7885.
39 B. Chen and G. Qian, Metal-Organic Frameworks for Photonics Applications, Springer Berlin Heidelberg, 2014.
40 S. Brunauer, L. S. Deming, W. E. Deming and E. Teller, J. Am. Chem. Soc., 1940, 62, 1723-1732.
41 K. D. Vogiatzis, W. Klopper and J. Friedrich, J. Chem. Theory Comput., 2015, 11, 1574-1584.
42 J. H. Cavka, S. Jakobsen, U. Olsbye, N. Guillou, C. Lamberti, S. Bordiga and K. P. Lillerud, J. Am. Chem. Soc., 2008, 130, 13850-13851.

Graphical Abstract
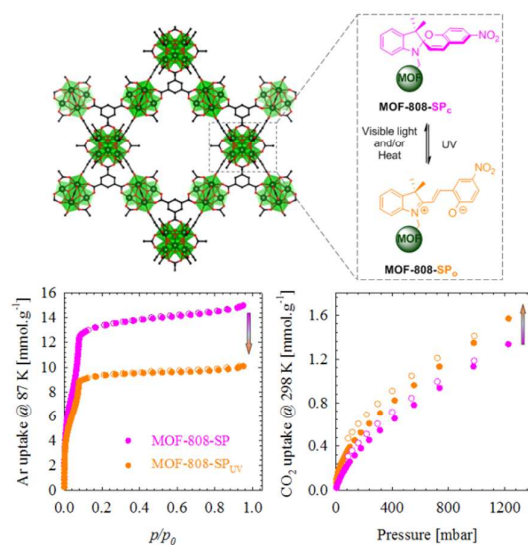
The first example of spiropyran (SP) functionalised metal-organic framework (MOF) was synthesised *via* a two-step post-synthesis modification of the Zr-oxo nodes in MOF-808. The resulting MOF-808-SP showed photoresponsive surface area, pore volume and CO_2 uptake.